RSC Advances

ROYAL SOCIETY OF CHEMISTRY

www.rsc.org/advances

Journal Name

ARTICLE

Zinc oxide Quantum Dots: Multifunctional candidates for arresting the C2C12 cancer cells and their role towards Caspase 3 and 7 genes

Received 00th January 20xx,
Accepted 00th January 20xx

DOI: 10.1039/x0xx00000x

www.rsc.org/

Rizwan Wahab[a,b*], Farheen Khan[c], You bing Yang[d], I.H.Hwang[e], Hyung-Shik Shin[f], Javed Ahmad[a,b] Sourabh Dwivedi[g], Shams T. Khan[a,b], Maqsood A. Siddiqui[a,b], Quaiser Saquib[a,b], Javed Musarrat[g], Abdulaziz A. Al-Khedhairy[a], Yogendra K. Mishra[h], and Bahy A. Ali[a,b]

Recently, nanoscale (<100 nm) inorganic materials, especially spherical shaped zinc oxide (ZnO-QDs) have received significant attention from broad community because of their potential utalizations in various technologies. Due to their large surface to volume (S/V) ratio contributions and extremely high reactivities, they can easily penetrate in various biological identities, like cells, proteins and hence can sense, diagnose and cure different biological systems. The present study describes the simple synthesis of crystalline ZnO-QDs via solution process and C2C12 myoblast cancer cells have been treated with different doses of ZnO-QDs at diffrent incubation (24, 48, 72 and 96 h) time. The rate of inhibition of cells was observed with MTT assay whereas morphology of cells was observed via confocal microscopy (CLSM). The MTT and CLSM investigations confirmed that with increase in the incubation time, the population density of cancer cells was decreased when treated with ZnO-QDs. The dose dependent apoptosis correlated intracellular production of reactive oxygen species (ROS) from C2C12 cancer cells was also measured in presence of ZnO-QDs. Apart from this, the effect/apoptosis of these QDs were also checked in presence of candidate genes such as caspase 3/7 with GAPDH. The Reverse transcription polymerase chain reacion (RT-PCR) analysis demonstrates the up-regulation of caspase 3/7 genes in cells subsequently treated with ZnO-QDs at low and high concentrations.

Introduction

Cancer disease is currently a very major issue in the society because of several deaths and the biomedical society is still looking for an appropriate alternative, which can kill cancer cells but at the same time it must be biocompatible so that normal and healthy cells remain unaffected. Recent developments in nanotechnology have provided new platforms of different kinds of nanostructures, which can be effectively used in biomedical engineering for various treatments. Owing to their S/V ratio in nanoscale region, these nanostructures exhibit extraordinary physical and chemical features, which enable them as potential building blocks for several multifunctional applications in different disciplines and particularly in biomedical field. For example very small nanostructures (~1-100 nm) can be effectively utilized in identify and cure of diverse categories of cancers[1] Different nanostructures find potential role for the detection of DNA, intracellular labeling, drug delivery, blocking viral entry into the cells, cancer targeting and imaging etc.[2-11] Also they are heavily utilized in cell and molecular biology, as markers and probes, for tissue engineering, for clinical bio-analytical diagnostics and therapeutics.[11-12] Nanostructures of metal oxides are very particular which are significantly used by industries for making several products in the market for day today life, e.g., cosmetics, catalysts, fillers and drug carriers.[13] Among various metal oxides, zinc oxide nano structures has drawn special attention for the materials scientist due to its bio compatible nature, low cost, easy to process and has already shown potentials applications in various fields such as sun screens, photocatalysis, cosmetic products, optoelectronic devices, etc.[14-16] In this regards, ZnO nanostructures, which have very small size (diameter <10 nm), are known as quantum dots (QDs), and are particularly very important because of their very high S/V ratio and

[a] Zoology Department, College of Science, King Saud University, Riyadh 11451, Saudi Arabia, *E-mail: rwahab05@gmail.com, rwahab@ksu.edu.sa; Tel: +966-536023284.
[b] Al-Jeraisy, Chair for DNA Research, Department of Zoology, College of Science, King Saud University, Riyadh 11451, Saudi Arabia
[c] Department of Chemistry, Aligarh Muslim University, Aligarh 202002 U.P. India
[d] Animal Science & Technology College, Henan University of Science and Technology, China
[e] Department of Animal Resources and Biotechnology, Chonbuk National University, Jeonju 561-756, Republic of Korea
[f] Energy Materials & Surface Science Laboratory, Solar Energy Research Center, School of Chemical Engineering, Chonbuk National University, Jeonju 561-756, Republic of Korea
[g] Department of Agricultural Microbiology, Faculty of Agricultural Sciences, Aligarh Muslim University, Aligarh 202002, India.
[h] Institute for Materials Science, Functional Nanomaterials University of Kiel, Kaiser Str. 2, 24143 Kiel, Germany.

†Electronic Supplementary Information (ESI) available: [details of any supplementary information available should be included here]. See DOI: 10.1039/x0xx00000x

therefore having high reactivity. Being from direct semiconductor family and with bandgap (~3.37 eV) similar to that of TiO_2 (~3.23 eV), ZnO-QDs include extraordinary fluorescent features helpful for identification or treatment. Because of very small diameter (<10 nm) these ZnO-QDs can easily penetrate into cells, viruses, proteins and other biological identities. ZnO-QDs are also superior to conventional organic based nanomaterials because of their high durability, chemically stable, easy to synthesize, least cytotoxicity, more selectivity, heat resistant etc.[17] In addition, ZnO nano structures offer unique feature of strong photosensitizing (PS) behaviour, which can be very useful in various photodynamic and skin care therapies, because of these ultrasmall quantum size.[18-20] The QDs are constrained on the upper part of stratum corneum, which provides effective optical response affected via UV-light.[21] These QDs exhibit the ability to reduce the growth of cancer cells due to cytotoxic nature. In this context, muscle cells provide an excellent model to evaluate the functionality of candidate genes of caspase series, which are the family of cysteine aspartate-specific with 14 members. The caspases plays an important role in cell inflammation or apoptosis and are categories in three different classes, which depend on their character.[22] In process of apoptosis caspases are further subdivided into initiator (8, 9, 10 and 11), whereas the effector caspase (3, 6 and 7) are depends on the location of cell death pathway.[22] The effector caspases (3, 6 and 7) are responsible for the interruption in cells after initiation of apoptosis. It catalyses the whole cells and damage the cellular proteins, which is a major reason of cellular death, and are accountable for disordering the cell as apoptosis process initiates. Caspase also targets caspase-activated DNase.[23-24]

Here we report very promising activity of highly crystalline ZnO-QDs against myoblast C2C12 cancer cells. The effective inhibition in growth of cancer cells with ZnO-QDs at dose dependent manner have been analyzed against C2C12 cells for the first time. The used ZnO-QDs were synthesized by soft chemical non-aqueous solution process which facilitates a simple and cost effective synthesis of highly crystalline quality of ZnO-QDs in large amounts. The effect/apoptosis of ZnO-QDs were also validated their toxic behavior against cancer cells in presence of candidate genes such as caspase 3 and caspase 7 with GAPDH genes. The process of ZnO-QDs interaction to cancer cells is also discussed as illustration.

Materials and Methods

Experimental

Synthesis of ZnO-QDs

For the formation of ZnO-QDs, precursor zinc acetate di-hydrate ($Zn(AC_2)_2.2H_2O$, 0.3 M) and n-propyl amine (CH_3-$(CH_2)_2$-NH_2) (20 mL) were mixed in 100 ml of methanol and stirred for 30 min. The chemicals related to the formation of QDs such as zinc acetate di-hydrate and n-propyl amine were purchased from Aldrich Chemical Co. Ltd and used without further purification. The pH of the prepared solution was observed at 8.39 by the pH meter (Cole parmer, U.K). The mixture of zinc acetate di-hydrate ($Zn(AC_2)_2.2H_2O$, 0.3 M) and n-propyl amine was shifted to a three necked refluxing flask and was refluxed at ~65°C for 9 h. After the complete refluxing process, white product was air cooled at room temperature. The white product was transferred to a centrifugation tube to remove the organic synthetic impurities via centrifugation (4000 rpm/min for 10 min, FLETA 5, Hamlin Sci ind. co. Ltd, U.K) process. The achieved white product was washed again and again with alcohol (methanol (MeOH), ethanol (EtOH)) and acetone, and dried in petridish at room temperature.

Characterization of ZnO-QDs

The dried white powder sample was characterized in terms of their structural and chemical properties. The structural observations of white powder were made by Field emission scanning electron microscopy (FESEM, Hitachi S-4700, Japan) and transmission electron microscopy (TEM, 200 keV, Jeol JSM 2010, Japan)). The crystallinity and phases of the white powder was characterized by an X-ray powder diffractometer (XRD, Rigaku, Japan) with used radiation $Cu_{K\alpha}$ (λ= 1.54 178 Å) in range of 20-65° with 6°/min scanning speed.

XRD **(Fig.S1(a)†)** shows the diffraction peaks in the pattern indexed as the hexagonal zinc oxide with lattice constants a= 3.249 and c=5.206 Å, and well matched with the accessible Joint Committee on Powder Diffraction Standards (JCPDS card No. 36-1451) of formed QDs. The particle size of grown QDs was also calculated with well-known Scherer formula with FWHM of XRD pattern, and the value of major peaks such as <1010>, <0002>, <1011>, <1012>, <1120>, <1013> obtained at 32.08, 34.82, 36.65, 47.94°, 57.00 and 63.26° respectively, were presented (**ESI,Table S1†**) and it shows that the dimension of particles are very small.[25-27]

$$D = \frac{0.9\,\lambda}{\beta \cos\theta}$$

Where λ is the wavelength of X-ray radiation source, β is full-width at half-maximum in [FWHM] radians, θ is Bragg's diffraction angle. The calculation was measured with the help of Gaussian lorentzian fitting Program. The mean value of particle sizes is ~7-8 nm. The chemical functional property of the grown QDs of white powder was characterized by Fourier transform infrared (FTIR, Perkin Elmer, U.S.A) spectroscopy in the range of 4000-400 cm^{-1}. In addition to these observations, the optical properties of QDs were also analysed at room temperature via UV-visible (Labomed, Model UV D-2950, in the range of 200-1000 nm) and photoluminescence (PL) spectroscopy with the He-Cd (325 nm) laser line as the exciton source in the range between 350-650 nm.

Binding Studies of ZnO-QDs with HSA Protein

Binding Studies of HSA with ZnO-QDs

The fluorescence quenching titration at increasing HSA to ZnO-QDs molar ratios has been performed. Briefly, at fixed concentration of HSA (3 μM) with various concentrations of ZnO-QDs (5-50 μM) were added in 10 mM Tris-HCl buffer at

an ambient temperature. The spectra of fluorescence were recorded under subdued light. Fluorescence measurements were carried out on a Shimadzu spectrofluorophotometer (model RF5301PC) equipped with RF 530 XPC instrument control software, using a quartz cell of 1 cm path length. The excitation and emission slits were set at 3 nm and 10 nm, respectively. The excitation and emission wave lengths at which the HSA fluorescence recorded were 280 nm and 330 nm, respectively. ZnO-QDs alone don't exhibit fluorescence at this wavelength range. Fluorescence quenching in terms of the quenching constant was determined following the Stern-Volmer Eq.[28] The slope of the double-logarithm plot (Log [(Fo-F)/(F-F∞)] versus Log [ZnO-QDs] in linear range provided number of equivalent binding sites (n) however, the value of Log [ZnO-QDs] at Log [(F0- F)/(F-F∞)] = 0 is equal to the negative logarithm of the binding constant (Ka).[28-29]

Cell culture

The cancer cells (C2C12) were procured from American Type culture collection (ATCC-CRL 1772; Bethesda, MD) and thawed at 37^{o}C in a water bath for ~2-3 min. The thawed cells were mixed with dulbecco's modified eagle's medium (DMEM) and centrifuged the cells for 4 min. The supernatant solution was discarded from the centrifuge tube and cells were transfered in 75 mm^2 area of volume bottles and were cultured in growth medium DMEM containing 10% fetal bovine serum (FBS), with antibiotics (streptopenicillin, and amphotericin B solution, 10 mL/lit each, sigma) in a humidified incubator at 37^{o}C with 5% CO_2 and 95% O_2 environment and washed with dulbecco's phosphate buffer (DPBS) solution. The medium was refilled every other day and the number of cells were observed daily and counted by haemocytometer and subcultured after it reached 50% confluence.

In vitro cell growth inhibition assay (MTT assay)

The MTT assay was used to check the percentage of viable cells via cell proliferation kit I (MTT, provided by ROCHE, Ltd, U.S.A) as per the detailed directions. Briefly, the cell lines were seeded into 96-well plates at 5 × 10^3 cell/well and incubated the plate for overnight at 37^{o}C in a humidified incubator. The C2C12 cells were incubated with different concentration of ZnO-QDs and returned to the incubator for 24, 48, 72 and 96 h. The MTT (3-(4, 5-dimethyl thiazol-2-yl)-2, 5-diphenyl tetrazolium bromide) solution (10 µL/well) was mixed with DMEM. The stored stock MTT solution was added to the control and treated with ZnO-QDs, cell samples and again incubated at 37^{o}C for 4 h. After the incubation, the samples were removed from incubator and mixed with solubilizing buffer (100 µL/well) solution, a purple color visible at this stage and deepen over pipetting. The control and treated samples were again incubated for overnight to ensure the formazan precipitate was dissolved. The measurement of MTT assay was analyzed with Elisa Reader (Bio-Rad) at 570 nm. The UV-irradiation provided by the deuterium and Xenon lamp. The percentage (%) of viable cells can be calculated as follows:

% Viability = [(total cells-viable cells)/total cells] × 100

Or

% Viability = OD (optical densities) in sample well /OD in control well × 100

MTT Assay

Seeding of cells in 96-well plate (5×10^3 cells/well)

↓ 24 h

Treatment of cells with prepared ZnO-QDs

↓ 24 h

Add MTT solution (10-20 µL to each well)

↓ 3 h

Discard media and add solublising buffer solution (100 µL) to each well

↓ Store overnight in 37 ^{o}C incubator

Read at 570 nm (ELISA reader) or store plate at -20^{o}C

Measurement of reactive oxygen species (ROS)

Intracellular production of ROS was measured using 2,7-dichlorofluorescein diacetate (DCFH-DA) as described by Wang and Joseph.[30] The DCFH-DA passively enters the cell, where it reacts with ROS to form the highly fluorescent compound dichlorofluorescein (DCF). In brief, 10 mM DCFH-DA stock solution (in MeOH) was diluted in culture medium without serum or another additive to yield a 100 µM working solution. C2C12 cancer cells were treated with ZnO-QDs on different concentrations (10, 100 and 200 µg/mL) for 24 h. At the end of exposure, cells were washed twice with buffer and then incubated in 1 mL of working solution of DCFH-DA at 37^{o}C for 30 min. Cells were centrifuged for 10 min and 200 µL supernatant was transferred to a 96-well plate. The fluorescence intensity was recorded at an excitation wave length of 485 nm and emission wavelength of 525 nm.

Confocal microscopy (CSLM) measurement

For quantitative study related to C2C12 cells and QDs, grown into a specialized confocal disk at 5 × 10^3 cell/well and it incubated with QDs at different incubation period (24, 48, 72 and 96 h) at 37^{o}C in a humidified environment. When the cells reached at 50% confluence, the media was removed from confocal disk and add DPBS (200 µL) solution, shaked well slightly and removed the DPBS from the confocal disk. The cells were fixed with using ethanol (70%, 200 µL) and to keep the solution for 10 min for the complete fixation. The incubated cells were again washed with using DPBS slightly shaked and completely removed the media from the disk. Afterward, cells were stained with propidium iodide [PI] (50 µL (PI) + 150 µL (DPBS)] solution and again incubate at 37^{o}C for 30 min in an incubator and wash with DPBS buffer. The stained cells were covered with glass cover slip for the microscopic observation.

Total RNA extraction from cultured C2C12 cells

Total RNA was extracted from C2C12 cells after various treatments for set periods of time using Trizol (sigma) according to the manufacturer's protocol. The purity of the total RNA was assessed by the ratio of optical density at 260 nm to 280 nm (acceptable values being between 1.6 and 2.1). First strand cDNA was synthesized from 1 µg of the total RNA using the M-MLV Reverse transcriptase with the anchored oligo d(T)12-18 primer. Real-time PCR was performed using a cDNA equivalent of 10 ng of total RNA from each sample with primers specific for caspase 3 and caspase 7 genes with a housekeeping gene GAPDH (**ESI, Table S2†**). The reaction was carried out in 10µL using SsoFastTM EvaGreen®Supermix (Bio-Rad) according to the manufacturers' instructions. Relative ratios were calculated based on the $2^{-\Delta\Delta CT}$ method. [31] PCR was monitored using the CFX96TM Real-Time PCR Detection Systems (Bio-Rad). (For detail information please see the supplementary information)

Statistical analysis

The obtained data is expressed as a mean ± SD. Statistical analysis was performed by student T-tests. Results were considered significant when $P < 0.05$.

Results

Morphological Invistigation

Detailed investigations of synthesized ZnO-QDs in terms of morphology and crystalline quality have been performed and the corresponding observations are demonstrated (Fig.1). Fig.1(a) & (b) illustrates the low and high magnified FESEM pictures of QDs. It is very clear from FESEM images that the ZnO-QDs are in spherical shape with gathered form and a closer look reveals their diameters to be in the range of 7-8 nm. To confirm the morphology and crystalline quality, these ZnO-QDs were investigated in detail inside TEM and their corresponding observations are demonstrated in Fig.1(c-d). In agreement with FESEM results, TEM observations also confirmed that these QDs exhibit almost spherical geometry with diameter about 7-8 nm (Fig.1c). The HR-TEM investigation (Fig.1d) on these ZnO-QDs confirmed their hexagonal wurtzite crystal structures with lattice constant around 0.265 nm (a axis) which was also found to be in close consistent with selected area electron diffraction (SAED) studies (inset in Fig.1d). Both TEM and FESEM observations are clearly consistent with the XRD analysis and denote that the synthesized QDs are single crystalline in nature (**ESI, Fig.S1a†**). [25-27] Since several chemicals were involved during synthesis, these ZnO-QDs were studied using FTIR spectroscopy to investigate if any chemical residue remained after the synthesis process. The FTIR spectrum (Fig.1e) confirms the fingerprints of $Zn(Ac_2).2H_2O$) and n-propylamine, which were used to synthesize these ZnO-QDs. The large and shallow peak ranges from 3200-3600 cm^{-1} corresponds to the water molecule whereas the sharp peaks centered at 1585 cm^{-1} and 1405 cm^{-1} are associated with C=O stretching from zinc acetate. [32-35] A curved and flat peak around 433 cm^{-1} in FTIR spectrum represents the formation of ZnO-QDs.

These ZnO-QDs were dispersed in deionized water (DW) and corresponding UV-visible spectrum (**ESI,Fig.S1b†**) also shows broad band absorption around 362 nm (3.42 eV), near to 1s–1s electron transition (3.37eV) from ZnO-QDs. [32-35] Apart from this, luminescent properties of these ZnO-QDs (at room temp) were investigated using PL spectroscopy and corresponding PL spectrum is presented (**ESI, Fig.S1c†**). A very sharp and intense PL peak has been observed at around 398 nm in the UV region which is mainly due to excitons however no peak has been observed in the green region confirming the high quality of these ZnO-QDs. [36] Normally a green peak is also expected in PL spectrum due to the present oxygen vacancies at the surface but in present case it seems that the oxygen vacancies are passivated due to used chemicals during synthesis. [36-41] In order to utilize them for cancer studies it was very necessary to investigate different properties of these ZnO-QDs and all observations confirmed that these QDs exhibit very high crystalline qualities.

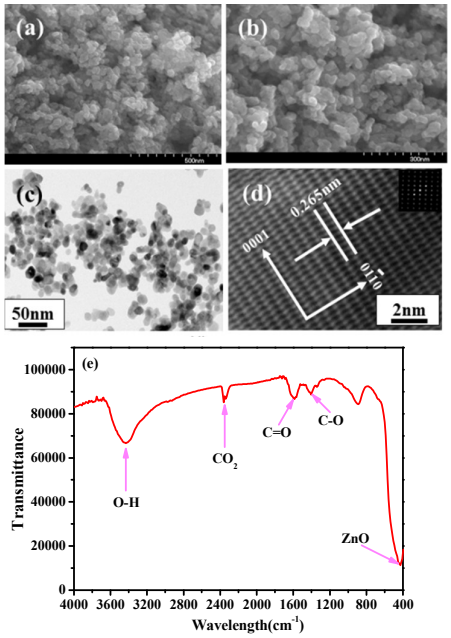

Fig.1. FESEM images of grown ZnO-QDs: (a) shows at low magnification whereas (b) presents the high magnification, (c) shows the low magnification TEM image of grown ZnO-QDs and (d) The HR-TEM image show the difference between two lattice fringes, which is ~0.265 nm. The corresponding SAED pattern (inset) consistent with the HR-TEM observations and it indicates the single crystallinity of the synthesized product, whereas (e) shows the FTIR spectroscopy of grown ZnO-QDs.

Based on synthesis, characterization and observations of the prepared QDs, a chemical formation process is also projected for the QDs. As per the material and methods, once in solution of $Zn(AC_2)_2.2H_2O$) mixed with n-propylamine under incessant stirring in MeOH, it forms a clear solution without precipitate at pH 8.39. Afterward six hours of refluxing at 65 ^oC, in the refluxing pot a white product ongoing to form and the refluxing process was completed in nine hours. As per the chemical observation (Fig.1e), amine ($-NH_2$) group decays

out from n-propylamine due to the breaking of hydrogen bonds and it reacts with the acetate (CH_3COO^-) group from $Zn(AC_2)_2.2H_2O$) initially, (eq.(1)) and the Zn^{2+} ions react with the propyl group and form a zinc complex ($ZnN\text{-}(CH_2)_2\text{-}CH_3$). It is assumed that as the temperature increases during the refluxing, the hydroxyl (OH^-) ions from MeOH react with the zinc complex and Zn^{2+} ions from the complex decompose, which then react to the hydroxyl (OH^-), form zinc hydroxide ($Zn(OH)_2$) (eq.(2), converted in to pure zinc oxide at higher refluxing temperature (ZnO) with water molecule (eq.3)). The intermediated species ($(CH_3)_2N\text{-}(CH_2)_2\text{-}CH_3$, CH_3COOH and H_2O molecule) from the reaction was pass out during centrifugation of the product.[32-35]

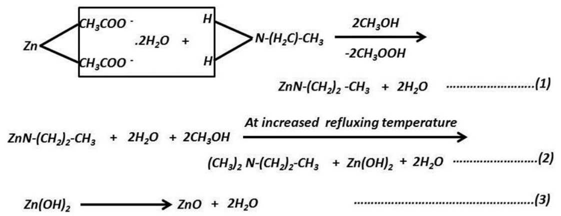

The interaction between HSA and ZnO-QDs was assessed at different concentration level, notable by fluorescence technique Fig.2. The fluorescence emission spectra were recorded with the ranges from 5 µM to 50 µM in five steps at 330 nm. In addition to increases the concentration of ZnO-QDs than fluorescence intensity gradually decreased, after quenching process HSA binds with ZnO-QDs and the fluorescence quenching constant (Ksv) calculated from Stern–Volmer equation (eq.4).[28]

$$F0/F = 1 + Ksv\,[ZnO\text{-}QDs] \quad \ldots\ldots(4)$$

Where F0 is absence fluorescence intensities, F is presence fluorescence intensities and K_{SV} Stern–Volmer quenching constant. A plot was established between F0/F versus [ZnO-QDs] (data not shown), obtained fluorescence quenching constant (Ksv = ~4.5×10^4 L mol^{-1}) by the slope of straight line. The linear line graph expressed that only one way quenching track for instance: static quenching or dynamic quenching was observed.[42] For applied eq.(5), the bonded macromolecules set as independently after reached at equilibrium point (at free and bound molecules). Moreover, when the molecules bind independently to a set of equivalent sites on a macromolecule, equilibrium between free and bound molecules are given by the equation mentioned below:[28]

$$\log [(F0 - F)/F] = \log K + n \log[Q] \quad \ldots\ldots(5)$$

where K is the binding constant. Thus, a plot of log (F0 -F)/F versus log [ZnO-QDs] can be used to determine K.

In culture process, proliferation of C2C12 cells interacted with ZnO-QDs at regular interval incubation times (24, 48, 72 and 96 h). Hereafter, observed first day mostly cells are single nucleate or mononucleate and third day cells reached at 50% confluence (**ESI, Fig.S2†**). Moreover, accommodated cells are directly connected with ZnO-QDs, which indicate that exact condition of cells, as to increases concentration of ZnO-QDs (10,100 and 200 µg/mL) with increases mortality of cancerous cells due to strong interaction between C2C12 cells and ZnO-QDs.

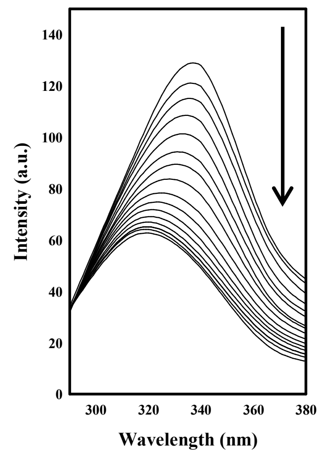

Fig 2. The Illustrative fluorescence spectra of ZnO-QDs in absence and presence of various concentration of HSA: shows the emission spectra of ZnO-QDs (50 µM) with varying HSA concentrations, i.e., 5, 10, 15, 20, 25, 30, 35, 40, 45 and 50 µM.

The MTT assay was used to examine the rate of proliferation of cells and toxicity caused with ZnO-QDs in cancer cells. This happens due to mitochondrial damage in cells and therefore decreased the efficiency in test. The MTT salt, which has yellow colour solution, reduces to purple formazan in mitochondria of living cells. To dissolve or solubilize a buffer solution usually DMSO is added to insoluble purple formazan product into a coloured solution. The absorbance of this colored solution was quantified by measuring at a certain wave length (usually 570 nm) by a spectrophotometer. The absorption maximum mainly depends on the employed solvent. The level of cytotoxicity or the percentage (%) viability was calculated as follows:

Viability = [(total cells-viable cells)/total cells] × 100

The acquired MTT assay informations displayed that at altered ZnO-QDs conc., exhibit constrain properties on the evolution of C2C12 cells. For endurance studies, cells were incubated with ZnO-QDs continuously and thereafter media was removed, cells density were determined via MTT assay with following addition of 10, 100 and 200 µg/mL of ZnO-QDs solution.[43-45] The ZnO-QDs with concentration of 10, 100, and 200 µg/mL of ZnO-QDs at 24 h killed 15.96, 12.53 and 0.79% respectively and for 48 h incubation cell decay behaviour was changed to 26.11, 15.97 and 5.12% for same ZnO-QDs concentration (i.e., for 10, 100 and 200 µg/mL) respectively. As the evolution time of cells increases in terms of desired conc., of ZnO-QDs, the cell death occurred corresponding to 72 h of incubation 34.53, 30.65 and 15.05% for 10, 100 and 200 µg/mL of, ZnO-QDs solution respectively.

The ZnO-QDs at concentration of 10, 100 and 200 µg/mL killed maximum cells, which were 67.55, 64.94 and 59.94% respectively (Fig.3).

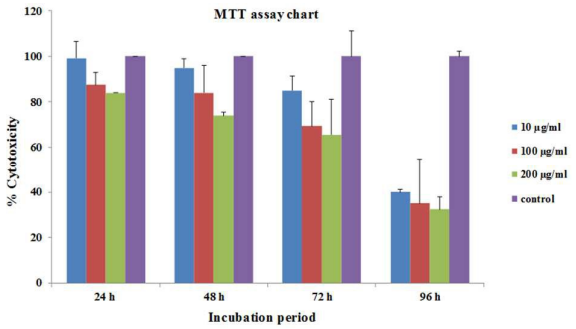

Fig 3. MTT assay chart at different incubation periods (24, 48, 72 and 96 h) with control solution.

ZnO-QDs used in the present study considerably transformed the prominence factor in terms of oxidant in C2C12 cancer cells. Higher production of intracellular reactive oxygen species (ROS) in ZnO-QDs treated cancer cells suggests that ROS generation and oxidative stress might be the primary mechanisms responsible for induced toxicity cancer cells due to ZnO-QDs. Current developments in cancer research suggest that a number of apoptotic stimuli share common mechanistic pathways characterized by the generation of ROS through oxidative stress. [46-47] ROS typically include the superoxide radical (O_2^-), hydrogen peroxide (H_2O_2), and hydroxyl radical (OH), which can cause damage to cellular components including DNA and proteins. The induced oxidative stress were evaluated with various concentration of ZnO-QDs (0, 10, 100 and 200 µg/mL) incubated for 24 h (Fig.4). At the end of treatment, ROS levels were determined, as described in materials and methods section. ROS Data represented are mean ± standard deviation of three identical experiments made in triplicate manner. The qualitative analysis of ROS generation revealed a concentration dependent increase 129, 178, 195% at 10, 100 and 200 µg/mL respectively in the fluorescence intensity of DCF in ZnO-QDs treated cells as compared to the untreated control cells (Fig.4). Considering the fluorescence intensity of untreated control cells as 100%, ZnO-QDs treated cells (in the concentration range of 0–100 µg/mL) were found to exhibit significantly higher fluorescence intensity of DCF ($p< 0.00 5$), respectively. [46-47]

Further the cell death with QDs were studied in detail using time dependent confocal scanning laser microscopy (CLSM) at different concentration of ZnO-QDs with control solution. The CLSM has property to provide the information of cells behaviour in wet environment. The cells were incubated with QDs at 37°C in an incubator with 5% CO_2 for 24, 48, 72 and 96 h and imposed using a CLSM with the staining solution PI and were observed at an excitation 543 and emission 620 nm wavelength (**ESI, Fig.S3†**). It was observed that the density of cell death at 24 h of incubation period is less (10 µg/mL) (Fig.5) which increases with rise concentration of ZnO-QDs from (100 µg/mL and 200 µg/mL).

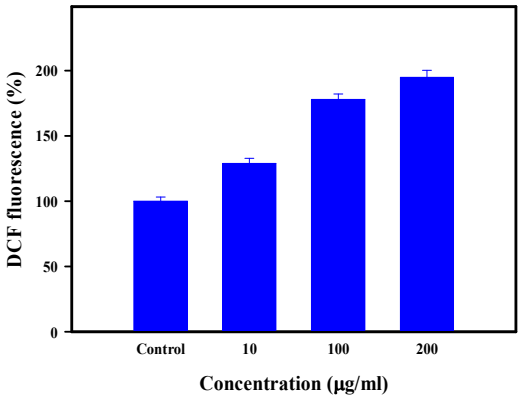

Fig 4. Induced oxidant generation in C2C12 cancer cells treated with various concentrations of ZnO-QDs (Control, 10, 100 and 200 µg/mL) incubated for 24 h.

Also with increase in incubation time (48 h), cells death density gets enhanced more and more which is shown in Fig. 5(a-h). It's very clear from the CLSM images that the toxicity of the cells mainly depends on the concentration of QDs and also with the incubation period. [48-49] From the CSLM observations, which are in close agreement with the MTT assay data (**fig.3** and **ESI, Fig.S3†**) and from both, it is very clear that the several hundred thousands of cells are accumulated in a spherical shape and the addition of these ZnO-QDs significantly decreases the density of cancerous cells (Fig.5). The control cells show the density of C2C12 cells (Fig.5) but as the doses of QDs treated in dose dependent (10, 100 and 200 µg/mL) and an optimized manner, cells density decrease. However, to understand the detailed mechanism and cause of induced toxicity in cancerous cells due to the QDs is under debate and it needs other required experiments which are under progress.

The previous cytotoxicity study with cancer cells with zinc oxide nanoparticles carried out by Wahab et al., strongly suggested that the exposure of C2C12 cells to NPs from lower to higher concentrations (5-100 µg/mL) respectively, incubated at 37°C for 24 h, that the cell growth is affected with increasing the concentration of NPs. [49] The present work is analogous to our previous work. [49] In another work, the gold nanoparticles, retarded the growth of C2C12 cells at dose dependent manner at a very low concentrations (0, 100, 500, 1000 ng/mL) incubated for 24 h at 37°C in presence of gold nanoparticles. [50] The mechanism of cell death was also explain with the utilization of CuO quantum dots on candidate genes such as caspases 3/7, which are responsible and key factor of apoptotic functions. The in vitro study of C2C12 with QDs described the effect of DNA, which are significantly decreases the viability of cells at dose (10-20 µg/mL) dependent manner. [51] On the basis of microscopic and previous published results, it can be summarized that the cytological potential of prepared QDs has remark-

able significance in this study at optimized concentration range.[51]

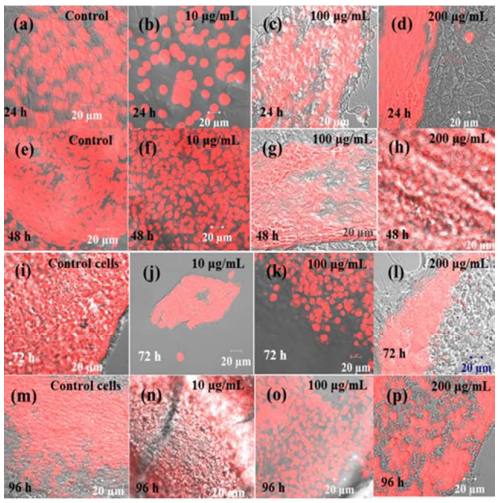

Fig 5. Confocal laser scanning microscopy (CLSM) images of C2C12 cells at different concentration (10,100, and 200 µg/mL) of ZnO-QDs with altered evolution (24, 48, 72 and 96 h) period.

The RT-PCR investigation was performed for to know the level of mRNA with markers (caspase 3/7) in presence of GAPDH gene against C2C12 cells. The cancer cells were interacted to QDs at low (10 µg/mL) and high concentration (200 µg/ mL) of QDs at 24 and 72 h incubation period. The obtained outcomes displayed that mRNA levels of markers (caspase 3/7) were significantly changed in C2C12 cells owed to QDs interaction (fig.6., p <0.05 for each). Genes expressions for caspase 3 with ZnO-QDs at low concentration at different incubation period (24 & 72 h) are 1.4 and 2.1 respectively. In case of caspase 7, the fold change of expression was upregulated to 2.7 at 24 h, whereas it was 4.7 fold high at 72 h incubation period. The Quantifiable RT-PCR outcomes revealed that QDs show up-regulated mRNA level of cell cycle checkpoint of caspase 3/7.[31] The influence of caspases 3/7 noticed in control cells, which resembled to the naturally growing cells due to incubation or aging. In reacted cells, activities of caspase 3/7 improved from 1.4-4.7 fold (p<0.05) over basal levels, which signifies an initiation of caspases in C2C12 cells reacted with QDs.[31] The change in gene expression was compared with an untreated sample as a control or a signature control for the knockdown data. From the statistical graph (Fig. 6) it's very clear, that ZnO-QDs exhibit toxic nature with respect to the growth of cancer cells. The apoptosis in cell is increased as the concentration of QDs is increases. The up regulation denotes the apoptosis caused due to the interaction of QDs. Similar observation have been obtained in case of caspase 7 interactions at 24 and 72 h incubations. In case of caspase 7 gene expression, at low concentration of ZnO-QDs incubated at 24 h, express two fold change were (2.0, 2.1 for 24 h incubation periods) apoptosis whereas at higher concentration and higher incubation period (72 h), apoptosis changes to 6 fold (6.6) (Fig 6).

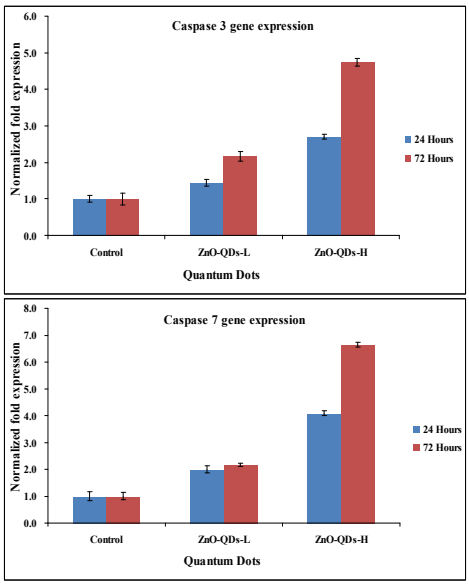

Fig 6. The mRNA Expression of C2C12 Cells with Caspase 3/7 and housekeeping GAPDH genes in presence of ZnO-QDs at low (10 µg/ mL, ZnO-QDs-L) and high (200 µg/mL, ZnO-QDs-H) concentration. Experiments were performed in triplicate manner (p <0.05).

3.2. Discussion

The synthesis of QDs (<10 nm) from precursor of ZnO is very much important aspect because they exhibit the potential of industrial applications in various technical areas such as, solar cells, UV light emitters, gas/chemical sensors; trans parent conductors, optoelectronic, etc. Recently, the utilization range of ZnO-QDs has been expanded to biomedical engineering too because of their large S/V ratio, enhanced catalytic, and biocompatibility.[14,32-35] Their very small nanoscale size makes them noticeable and valuable material further biorelated applications, for example in drug delivery, cell and DNA repair/damage, etc.[6-7, 14, 32-35] The ZnO-QDs in present were prepared via a non-aqueous solution process. The XRD results confirmed that they are single crystalline in nature and their dimension is in the quantum size range (<10 nm). The TEM revealed their nearly spherical shape and smooth surface and the average diameter is about 7-8 nm in agreement with XRD analysis. The HR-TEM study also supported their crystalline nature average lattice spacing ~0.265 nm, which is identical to pure wurtzite ZnO[6-7, 14, 32-35]. The toxicity of grown QDs in cultured medium of cancer cells, was determined by using MTT assay analysis. From the detailed observation of MTT assay, it is clear that these small ZnO-QDs (dia~7-8 nm) exhibit remarkable effect against C2C12 cells (at low doses of 10, 100 and 200 µg/mL in dose dependent manner) in presence of control solution.[52] The cell toxicity was also observed in terms of apoptosis and cell death due to QDs was also observed with the existing ROS at dose dependent manner (for 24 h incubation time). The apoptosis in C2C12 cells were analysed via RT-PCR utilized to analyse the mRNA levels of apoptotic markers

(e.g. caspase-3/7) in presence of QDs at low and high (10 µg/mL and 200 µg/mL) concentration for 24 h incubation. The observed expression data in both the cases (caspase-3/7 with ZnO-QDs) were accordingly up-regulated.[53] In the recent past, previous studies shows that the cytochrome c, binds to protease of apoptosis, which generally known as apoptosis of protease activating factor-1 (Apaf-1), forms a complex apoptosome. These apoptosomes have property to bind with procaspase-7 and causes their auto-activation through a conformational change. As caspase-7 initiated, it goes on to activate caspase-3, cleaves substrates at aspartate residues and activation of this proteolytic activity leads to apoptosis. The RT-PCR study supported that the QDs are significantly up-regulated with caspases-3/7 expression in proliferated cells. [54-56] On the basis of the finding and their observations, we have proposed a probable pictorial model for cytotoxic process of ZnO-QDs with C2C12 cells which is shown in Fig.7.

On the basis of previous literature [45] and observations, it can be postulates that the cytotoxicity caused through QDs/NPs, which depends on various parameters such as size, shape, chemical structure, stoichiometry of the QDs. The toxicity via QDs also affects the endocytic uptake of cells.[57] The QDs first attached on the surface of cancerous cells, which exhibit small pores. These pores form passages to enter the QDs on cancer cells (as schemated in Fig.7). Due to very small size of QDs, they exhibit the natural tendency to cross the upper layers of cancerous cells very easily as compared to other bigger size nanostructures. It is assumes that in cells, QDs are jointed with each particles and form aggregates, and these aggregates of QDs are responsible for the destruction of cell organelle for instance nucleus which have ~5-10 µm size and mitochondria, endoplasmic reticulum and nucleic acids are ~1-2 µm etc.[45-46] From the gene expression data (Fig.6) it is very clear that introduced QDs are responsible for controlling the proliferation and destroying the cell organelle of cancer cells. The dose dependent MTT and RT-PCR studies clearly demonstrate the apoptosis and cell death in cancer cells. The treatment also explains to sensitize C2C12 cells, by increasing the concentration of ZnO-QDs. The increased cell death caused with the dose dependent addition of ZnO-QDs at different incubation periods (**ESI, Fig.S3†,** Fig.4). From genetic (RNA extraction) studies (Fig.6), it is evident, that cells growth is significantly affected in presence of ZnO-QDs, which are mainly responsible for cell death. The cytotoxicity of the grown materials of ZnO-QDs was tested with MTT assay in grown cultured system.[44] The free radicals (FRs), which are generally produced in cultured cells interacted via solution of nanostructured materials and are responsible for to generate ROS. These FRs have property to inter into the outer wall of cells and it goes to inner wall of cell membrane. In cells enzymatic changes occurred when the FRs reacts with the cells organelle, which leads to damage or disorganization of cells.[45,49, 57] The previous works highlight that the nano structures have capability to induce ROS in cancer cells.[49] The mRNA levels of expression of caspase-3/7 in presence of ZnO-QDs in cancer cells have been examined. The RT-PCR results showed that the QDs, up-regulates the mRNA level of cell cycle checkpoint. The mRNA expressions and their actions of apoptotic gene caspase-3/7 were higher in QDs treated cells. The phenomena why the QDs are responsible to retards the proliferation rate of cells and their biochemical and enzymatic changes are under investigation and it needs further study to investigate the role of QDs against cancer cells.[57] In most of the published literature employed nano structures were either utilized toxic material or at higher concentration for the toxicity studies, which are difficult for human exposure. We may believe that the use of small sized structures (QDs of ZnO) at optimized/low concentration would be supportive to control the explosion of cancer cells due to biocompatible nature and have no adverse effect on the body. [58]

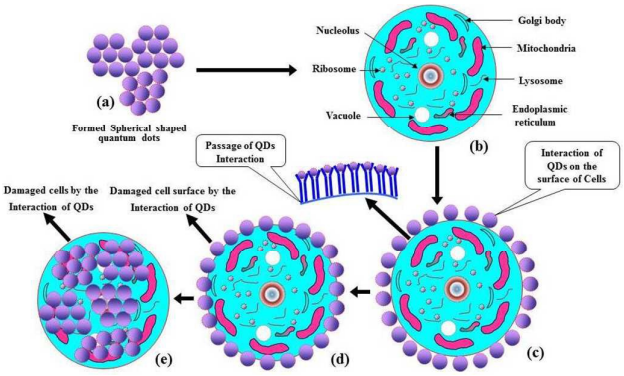

Fig 7. Possible proposed schematic mechanism for the interaction of ZnO-QDs against C2C12 and their cytological death.

4.0. Conclusion

In summary, the high crystalline qualities of ZnO-QDs with very uniform size distribution of QDs were successfully synthesized via solution process in a controlled manner. The synthesized ZnO-QDs were utilized for investigating their effect with respect to cancer cells (C2C12) and the results suggest that these QDs may be regarded as an effective new class of anticancer agent. It is examine that as the conc. of utilized QDs is lower their effect is much pronounced in comparison to larger amounts of QDs. The low concentrated ZnO-QDs seem to be entered easily into the cells pores and reacting significantly with the cells organelles, however when large concentration of QDs is utilized, self-agglomerations of QDs might hinder their effective entry into the cells and therefore reduced effect. The MTT, ROS and RT-PCR studies, clearly demonstrated that the treatment of QDs at dose dependent manner against C2C12 cells and retarded the growth of cancer cells. The main importance of our finding explores that the QDs of ZnO can be utilized as the effective anticancer agents at low concentration. Although, the detailed investigation relating to structure and their activity of QDs as well as their stability in cells under appropriate conditions is required. The comprehensive observations might be helpful in designing more effective anticancer agents for therapeutic use. By these studies, it is confirmed

that the QDs are safe and effective candidates to reduce the growth of cancer cells for the larger scale applications. The apoptosis correlated ROS production was also quantified in C2C12 cancer cells with QDs at various doses. The genetic caspase studies also revealed that the cells growth is strongly affected due to ZnO-QDs which are responsible for cell death.

Conflict of interest statement

The authors declare that there are no conflicts of interest.

Acknowledgement

This project was financially supported by King Saud University, Vice Deanship of Research Chairs.

References

1. X.Michalet, F.F. Pinaud, L.A. Bentolila, J.M. Tsay, S.Doose, J.J.Li, S.Sundaresan, A.M. Wu, S.S. Gambhir, S.Weiss, *Science,* 2005, **307**, 538-544.
2. K.Riehemann, S.W.Schneider, T.A. Luger, B.Godin, M. Ferr ari and H. Fuchs, *Angewandte Chemie International Edition*.2009, **48 (5),** 872-897.
3. Y.K.Mishra, R. Adelung, C. Röhl, D. Shukla, F.Spors, V. Tiwari, *Antiviral Research* 2011, **92(2)**, 305-312.
4. T.E. Antoine, Y.K. Mishra, J.Trigilio, V.Tiwari, R.Adelung, D Shukla, *Antiviral Research* 2012, **96**, 363-375.
5. H.Papavlassopoulos, Y.K. Mishra, S. Kaps, I. Paulowicz, R. Abdelaziz, M. Elbahri, E.Maser, R.Adelung, C.Rohl, *PLOS ONE,* 2014, **9(1)**, e84983.
6. R.Wahab, N.K.Kaushik, N.Kaushik, E.H.Choi, A.Umar, S. D wivedi, J.Musarrat, A.A.Al-Khedhairy. *J Biomed Nanotech* 2013, **9**, 1181-1189.
7. R.Wahab, N.K.Kaushik, A.K.Verma, A.Mishra, I.H.Hwang, Y.B.Yang, H.S.Shin, Y.S.Kim, *J Biological Inorg Chem* 2011, **16(3)**, 431-442.
8. Y. Weizmann, F. Patolsky, E. Katz, I.Willner, *J Am Chem. Soc*. 2003, **125**, 3452-3454.
9. H.T. Song, J.S. Choi, Y.M. Huh, S.J. Kim, Y.W. Jun, J.S. Suh, J.W. Cheon, *J. Am Chem Soc* 2005, **127(28)**, 9992-9993.
10. M. Mahmoudi, A. Simchi, M. Imani, U.O. Hafeli. *J Phys Chem C.* 2009, **113(19)**, 8124-8.
11. J.M. Laval, P.E. Mazeran, D.Thomas. *Analyst* 1999, **125**, 29-33.
12. T.A.Desai, *Medical Engg & Physics* 2001, **22(9)**, 595-606.
13. R.H. Hurt, M. Monthioux, A. Kane, *Carbon* 2006, **44(6)**, 1028-1033.
14. R. Wahab, Y.S. Kim, H.S. Shin, *Current Appl Phys* 2011, **11**, 334-340.
15. H.H. Wang, C.S. Xie, W. Zhang, S.Z. Cai, Z.H. Yang, Y.H. Gui. *J Hazard Mater* 2007, **141**, 645-652.
16. S.S. Hong, T.H.Joo, II.W. Park, Y.H. Jun, G.C. Yi, *Appl Phys Lett* 2003, **83**, 4157-4159.
17. D. Bechet, P. Couleaud, C. Frochot, M.L. Viriot, F.Guillem in and M.B. Heyob. *Trends in Biotechnology* 2008, **26**,612 -621.
18. T.Jamieson, R.Bakhshi, D. Petrova, R.Pocock, M.Imani, A. H.Seifalian. 2007, **28**, 4717-4732.
19. K.Y.Kim. *Nanomedicine: Nanotech, Biology and Med.* 2007, **3**, 103-110.
20. Y.Chen, D.M. Bangall, H.Koh, K.P.Hiraga, K.Z. Zhu, T. Yao, *J Appl Phys* 1998, **84**, 3912-3918.
21. G.M. Murphy, *Photoimmunol. Photomed*. 1999, **15**, 34-36.
22. W.C. Earnshaw, L.M. Martins and S.H. Kaufmann. *Annu Rev Biochem* 1999, **68**, 383-424.
23. M. Enari, H. Sakahira, H. Yokoyana, K. Okawa, A. Iwama tsu and S.Nagata, *Nature* 1998, **391(6662)**, 43-50.
24. H. Sakahira, M. Enari and S. Nagata. *Nature*. 1998, **391 (6662)**, 96-99.
25. Q. Zhang, T.P. Chou, B. Russo S.A. Jenekhe, G.Z. Cao. *Angew. Chem. Int Ed.* 2008, **47(13)**, 2402-2406.
26. G. Ambrožič, S.D. Škapin, M.Zigon, and Z.C. Orel, *J Coll and Inter Scie* 2010, **346(2)**, 317-323.
27. B.D. Cullity. *Addison-Wesley, Reading MA*, 1978, 102.
28. J.R. Lakowicz, *3rd ed., Springer*, 2006, 278-282.
29. K.L. Henderson, I.B. Belden, I.R. Coats. *Environ. Sci.Tech* 2007, **41**, 4084-4089.
30. H. Wang and J. A. Joseph. *Free Radical Bio.Med* 1999, **27**, 612-616.
31. M.W. Pfaffl. *Nucleic Acids Res* 2001, **29(9)**, e45.
32. R. Wahab. S.G. Ansari, Y.S. Kim, H.K. Seo, G.S. Kim, G. Khang, H.S. Shin, Mater. Res.Bull. 2007, **42(9)**, 1640-1648.
33. R. Wahab, S.G. Ansari, Y.S. Kim, H.K. Seo, H.S. Shin, *Appl. Surf. Sci.* 2007, **253**, 7622-7626.
34. R. Wahab, S.G. Ansari, Y.S. Kim, G. Khang, and H.S. Shin. *Appl Surf Sci* 2008, **254(7)**, 2037-2042.
35. R. Wahab, Y.S. Kim, I.H. Hwang, H.S. Shin, *Synth Metals*. 2009, **159**, 2443-2452.
36. X.Jin, M.Götz, S.Wille, Y.K.Mishra, R.Adelung, C.Zollfrank, *Adv Mater* 2013, **25(9)** 1342-1347.
37. W. Li, D.S. Mao, Z.H. Zheng, X. Wang, X.H. Liu, S.C. Zhu, Q.Li, J.F. Xu. *Surf. Coat. Technol*. 2000, **128**, 346-350.
38. S.A. Studenikin, N. Golego, M. Cocivera, *J Appl Phys* 1998, **84(4)**, 2287-2294.
39. B. Liu, H.C. Zeng. *J Am Chem Soc* 2003, **125(15)**, 4430-4431.
40. H.J. Egelhaaf, D. Oelkrug. *J Cryst Growth* 1996, **161**, 190-194.
41. S.K. Pardeshi, A.B. Patil, *J Mole Cat A: Chemical* 2009, **308**, 32-40.

42. J.L.Bresloff, D.M. Crothers, *Biochem*. 1981, **20(12)**, 3547-3553.

43. S. Ostrovsky, G. Kazimirsky, A. Gedanken, C. Brodie. *Nano Res.* 2009, **2(11)**, 882-890.

44. T. Mosmann, *J Immunol Methods*. 1983, **65**, 55-63.

45. E.Chang, N. Thekkek, W.W. Yu, V.L. Colvin, R. Drezek. *Small* 2006, **12**, 1412-1417.

46. R.R. Letfullin, C.B. Iversen, T.F. George, *Nanomed: Nano technology, Biology, and Medicine* 2011, **7(2)**, 137-145.

47. M.Ahamed, M. J. Akhtar, M. A. Siddiqui, J. Ahmad, J. Musarrat, A.A.Al-Khedhairy, M.S.Al-Salhi, and S.A. Alroka yan. *Toxicology* 2011, **283**, 101-108.

48. R.Wahab,Y.B.Yang, A.Umar, S.Singh, I.H.Hwang, H.S.Shin and Y.S. Kim, *J Biomed Nanotech* 2012, **8**, 424-431.

49. R.Wahab, S.Dwivedi, A.Umar, S.Singh, I.H.Hwang, H.S. Shin, J.Musarrat, A.A. Al-Khedhairy, Y.S. Kim, *J Biomed Nanotech* 2013, **9**, 441-449.

50. R.Wahab, S.Dwivedi, F.Khan, Y.K. Mishra, I.H. Hwang, H.S. Shin, J.Musarrat, A. A.Al-Khedhairy*, Colloids. Surface. B.* 2014, **123**, 664- 672.

51.T.Amna, H.V.Ba, M.Vaseem, M.S.Hassan, M.S.Khil, Y.B. Hahn, H.K.Lee, I.H.Hwang, *Appl Microbiol Biotechnol* 2013, **97(12)**, 5545-5553.

52. S.J.Soenen, B.Manshian, J.M.Montenegro, F.Amin, B. Meermann, T.Thiron, M. Cornelissen,F.Vanhaecke, S. Doak,W.J.Parak, S.D.Smedt and K. Braeckmans, *ACS Nano* 2012, **6(7)**, 5767-5783.

53. A.M.Alkilany, C.J. Murphy, *J Nanopart Res* 2010, **12(7)**, 2313-2333.

54. R.U.Jänicke, P.Ng, M.L.Sprengart, A.G. Porter, *J Biol Chem* 1998, **273(25)**, 15540-15545.

55. J.C.Timmer, G.S. Salvesen, *Cell Death Differ* 2007*,* **14**, 66-72.

56. W.C.Earnshaw, L.M.Martins, and S. H.Kaufmann. *Annu. Rev. Biochem.* 1999, **68**, 383-424.

57. L.K.Limbach, Y. Li, R.N. Grass, T.J. Brunner. M.A. Hinter mann, M. Muller, D. Gunther, W.J. Stark, *Environ. Sci. Technol* 2005, **39(23)**, 9370-9376.

58. S.M.Hussain, J.J.Schlager, *Oxf. J* 2009, **108**, 223-224.